Proceedings of 20th International Congress on Acoustics, ICA 2010

23–27 August 2010, Sydney, Australia

Acoustic Radiation of Friction-induced Pad-mode Instability in Disc Brake Squeal

S. Oberst*, J.C.S. Lai

Acoustics & Vibration Unit,
School of Engineering and Information Technology,
The University of New South Wales, Australian Defence Force Academy,
Canberra, ACT 2600, Australia

ABSTRACT

Since the early 1920s, disc brake squeal has been an issue for the automobile industry due to dissatisfied customer's complaints and the accompanying warranty costs. Despite a good deal of progress having been made in predicting brake squeal propensity, not all mechanisms are known and brake squeal remains unpredictable and highly fugitive. In recent years, research has been focused on brake squeal due to the mode-coupling type of instability, leaving out the primary friction-induced mechanisms such as stick-slip. In this paper, the acoustic radiation of simplified brake systems, in the form of a pad rubbing on both a plate and disc, is investigated. The radiation efficiency and acoustic power are calculated using the acoustic boundary element method, specifically ESI's Fast Multipole Solver (DFMM) implemented in VAOne. Results show that there exist some frequencies at which squeal occurs but which are predicted by the complex eigenvalue method. These frequencies do not correspond to the frequencies of the rotor modes and are here referred to as 'instantaneous' pad-modes causing a friction-induced instability. The frequencies of these instantaneous modes are dependent on the material properties of the pad and the contact conditions. Radiation efficiency due to pressure variations changes less, than due to friction coefficient variations. Further, it is shown, that pad-modes are acoustically relevant and especially active at lower pressures.

INTRODUCTION

Research on disc brake squeal has increased substantially in the past decade [1] because of continuing reductions in interior vehicle noise and the increasing number of noise-related warranty claims being lodged. Most customers perceive brake squeal to be an indication of a faulty brake system or are simply annoyed by it and likely to be dissatisfied with their automobiles. Hence, friction material suppliers allocate more than half their budgets to dealing with noise, vibration and harshness (NVH) problems [2] in very costly time consuming testing procedures [3]. According to Akay [4], up to US $1 billion was spent on NVH issues in North America in the early 2000s. As a consequence, there has been significant progress made in understanding the generation of brake squeal and in developing numerical methods for analysing its propensity as, for example, can be seen in recent reviews [5–12]. However, as pointed out by Oberst & Lai [1], the problem of predicting and reducing brake squeal propensity remains as challenging as ever. This is because the nature of brake squeal is fugitive, transient, and often non-repeatable due to its high dependency on a large number of interacting parameters, such as contact conditions, material properties and ever-changing operating conditions.

Mechanisms investigated so far which are thought to be responsible for brake squeal include stick-slip [13–15], negative gradient of friction coefficient with sliding velocity $\frac{\partial \mu_k}{\partial v_s}$ [16], sprag-slip [17], mode coupling or binary flutter [18], hammering [19], parametric resonances [20, 21] and moving loads [22]. Other mechanisms sometimes mentioned include thermo-elastic instability (TEI) [23, 24], viscous instability [25] and stick-slip-separation waves [26–28].

The brake rotor with its large surface area is a major sound radiator [29] and can be modelled as an annular disc. The governing equations originate from plate theory [30, 31] for which a circular structure with applied rotation is a special case and is found in research based on circular saws or computer hard drives [32]. In a first approximation, annular discs can be seen as plates [31] which are differentiated as being thin or thick. A review of thick plate theories has been written by [33] and a thick plate's particularly non-linear behaviour has been described by [30]. For circular saws, thin plate theory is often used but for a brake rotor, thick plate theory due to the influence of in-plane modes becomes more relevant, as systematically investigated in [34], with reference to brake squeal. However, these review articles cover only structural analyses. A comprehensive book, which also deals with the *acoustic properties* of plates and, among other structures, annular discs, has been written by [31]. However, as stated by [35], little is yet known concerning their acoustic radiation. The evolution in the analysis of sound radiation due to squeal by using a simplified brake rotor can be classified into three categories: circular plates, annular discs and brake rotors, as given in Table 1. Circular plates have a negligible inner radius; in practical investigations often with only a hole, to be fixed as, for instance, a saw blade. Enlarging the hole by increasing the inner radius leads to annular discs which can be either thin, as for a computer hard drive, or thick. Symmetrical structures such as discs have double-bending modes so-called doublets due to radial asymmetry [6]. These modes, with radial diameters, split into modes of the same shape, but with 90° phase difference and are called co-sine and sine modes, having the same natural frequency. Due to rotation the number of modal peaks found in the forced response spectrum increases caused by mode splitting, which means, the doublets

develop different frequencies [36–38]. Thick annular discs are good approximations of a brake rotor's cheeks and are able to display the similar pure out-of-plane/in-plane modes as a real brake rotor [35]. From Table 1, most brake squeal research has been directed towards the analysis of structural vibrations of discs and rotors. Only in recent years has the radiation of brake rotors been investigated by numerical methods in acoustics, [35, 39, 40]. Frictional contact and its effects on sound radiation have mostly been neglected for numerical analysis of brake squeal. By testing different materials on plates and plotting the radiation efficiency over the potential sound power level and the airborne sound power level a frictional sound map, has been developed [41, 42]. Only recently, an investigation into the sound radiation of a simplified brake system for unstable vibration modes predicted by the complex eigenvalue analysis (CEA) has been undertaken using the acoustic boundary element method (BEM) [43, 44].

In this paper, the sound radiation of simplified brake systems, in the form of firstly, a pad-on-plate and secondly, an annular disc in contact with an isotropic or anisotropic pad-on-disc is studied by analysing the effect of changes in pressure and friction coefficient on the radiated acoustic power and radiation efficiency. This complements the vibrational study performed on these structures in [65]. As guidelines for setting up the structural model and performing the acoustic calculations, the recommendations from [66] and the methods described in [67] are applied. The pad-on-plate system, as described by Chen [12], is used because it does only exhibit pure pad-mode instabilities and no interactions with the mode coupling of split modes [65]. The isotropic pad-on-disc system is analysed in terms of acoustic power by including global structural damping and variations in the number of constrained nodes, using stiffened and compliant boundary conditions (BC) [67]. Finally, the effect of material properties of the pad materials on the acoustic radiation of the anisotropic pad-on-disc system used in the structural analysis [65] is studied.

NUMERICAL MODELS

In this paper, three different models are used. In general, *plate*-models consist of a slider on a moving plate, similar to the analytical models used in [68, 69] but with elasticity and area contact. These models represent a simplified annular disc cut open and stretched to a plate. As previously analysed simplified brake systems are fcoussed on mode-coupling instability due to the merging of the split modes [43, 60, 44], this type of instability is not expected for a plate model due to the loss of its annular structure. *Disc*-models consist of a pad on a moving disc. In the following section, the four models studied are briefly described.

- *Plate*-models:
  - (I) *isotropic pad*: translational moving steel plate; variation: friction coefficient, pressure
  - (II) *transversely isotropic pad*: NA (studied in [65], but left out in the present paper)
- *Disc*-models:
  - (III) *isotropic pad*: rotating thick annular disc; variation: friction coefficients; material
  - (IV) *transversely isotropic pad*: isotropic steel back - plate; rotating thick annular disc; variation: friction coefficient, material constants with pressure

The form factor (size, geometrical features) remains the same for the isotropic/an-isotropic pad-on-plate/disc models except that, for the an-isotropic pad, a back-plate is attached to the lining material which results in higher out-of-plane stiffness. Since the total thickness remains the same, the lining thickness has to be reduced. Henceforth, the emphasis is on model I and model IV, as model I approximates an experiment performed

Table 1: Table of works related to radiation of discs and rotors. *BC*, Π, n and q, spl, μ, σ stand for boundary conditions, acoustic power level, number of nodal lines and radial diameters, sound pressure level, friction coefficient and acoustic radiation efficiency

Circular Plates	
Author	Findings
Irie et al. [45, 46] 1979/82	*vibration; plate* - clamped-free *BC* similar eigenvalues for radial thickness variation (linear, parabolic, exponential) - natural frequencies as function of disc parameters
Weisensel [45, 46] 1989	*vibration; plate/disc* - overview for stationary natural frequencies - covers different theories of elastic plates/discs
Rdzanek et al. [47–50] 2000 – 2003	*vibraion/radiation; plate/disc* - circular plate far simpler than annular disc - oscillating mutual active/ reactive Π vs kr
Annular Discs	
Author	Findings
Lee & Sing [51] 1994	*vibration/radiation; forced disc* - no change in σ up to $v_{rot} = 100Hz$ - axisymmetric radiate better asymmetric modes - multimodal excitation couples acoustic modes
Beslin & Nicolas [52] 1996	*vibration/radiation; forced disc* - rotating: stationary turn into rotating modes - rotating waves non-radiating or radiating
Cote et al. [53, 37] 1994/98	*radiation, forced disc* - theory of rotating (thin) plate - eigenfrequencies dependent on speed - rotation: modes with more nodal diameters and split modes at high frequency radiate better
Ewins [38] 2000	*vibration; discs* - axially/cyclically symmetry: phase-shifted doublets - axial symmetry lost: mode splitting - pad excitation equals multimodal excitation
Lee & Singh [54–56, 35, 39] 2002 – 2005	*vibration/radiation; forced disc* - thick better than thin plate theory - for radiation problem sufficient: structural mode synthesis, Rayleigh integral or cylindrical radiator - thick plate theory: modal coupling (*MC*) weak - hat-structure: coupling in-/out-of-plane modes - multi-mode excitation: *MC*, but weak effect on Π - annular disc: adequate in-&out-of-plane modes - Π high for coupled split modes or modes with same nodal diameter - low Π: in-plane modes - high Π: in-&out-of-plane coupling only if $n = q$
Kinkaid et al. [57, 58] 2004	*vibration; forced/pressurised disc* - vibration of simplified rotor in time domain - sliding: radial impuls with decceleration at low speed while sliding - bursts travel in contact patch non-constant speed - low speeds: circumferential & radial coupling strong
Loesche [59] 2009	*vibration; pressurised disc* - one side contact, simplified brake system as in [44] - area contributions in external acoustics show energy reflection effect due to geometry
Oberst & Lai [43, 60, 61] 2009	*vibration/radiation; forced/pressurised disc* - FE/BE analysis of unstable vibration modes - in vicinity of transition point highest spl - increased positive real part: spl not higher - aperiodic tori and intermittent chaos - Π oscillates and maximum at transition point - critical μ not confirmed by means of BEM
Brake Rotors	
Author	Findings
Flint & Hald [62] 2003	*full brake system* - increasing spl: $-$travelling wave - declining SPL: stationary wave, then $+$ travelling - Modal domain: standing wave has zero real part
Bea & Wickert [63], [7] 2000	*vibration; forced disc/rotor* - connection: annular disc/brake rotors - parameter study of hat-depth-ratio - disc& hat-structure: no pure disc-bending
Patching [64] 2006	*vibration/radiation; forced brake system* - assembled brake system: but no friction or pressure - peak of σ lower in frequency than rotor alone - stationary behaviour the same as rotor alone
Semilefendigil [40] 2006	*vibration/radiation; forced rotor* - brake rotor out-of-plane modes give $\sigma \in [0.4, 0.9]$ - in-plane σ small

by Chen [12] and model IV provides the opportunity to investigate the influence of the lining material properties due to the lining's compressibility under load on the acoustic radiation. In Figure 1(a), the pad-on-plate (II) and in (b) the pad-on-disc (IV) model are depicted. The isotropic material properties of pad-on-disc model I are modally updated via FEM to closely match three plate frequencies, 5.7, 8.2 and 11kHz, identified in the experiment of Chen [12]. For the elastic modulus and the Poisson's ratio, 210GPa and 0.305 are used, the density is calculated from the weights of the pin ($110g$) and the plate ($648g$) as 8025 and 7744kg/m^3.Thus, under free-free boundary conditions, the three *plate*-modes are found at $(p,q) = (1,1) = 5774.8Hz$, $(0,1) = 8083.3Hz$ and $(1,0) = 11044Hz$. p and q are the nodal lines in the longitudinal and transverse in-plane directions, respectively [70]. In order to investigate the influence of material property changes of the brake lining in model IV, data taken from Yuhas et al. [71] are given in Figure 2 and Tables 2 & 3 for 5 different pressures: $0.001, 0.5, 2.5, 5$ and 8MPa. The material points, $M_1 - M_4$, specify the elastic constants at each of the four pressures and are used for model IV. For all the other models, calculations are made either at a given pressure with a range of material properties or at given material properties with a range of pressures.

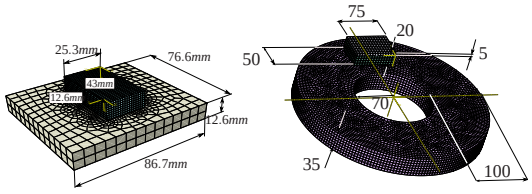

(a) (b)

Figure 1: (colour online) (a) isotropic pad-on-plate model (I) and (b) anisotropic pad-on-disc model (IV)

Table 2: Material parameters for models I-IV

	Models/ No. Elements	Constant	Plate/Disc	Lining	Backplate
isotropic	**I**/6,312 **III**/26,153	E GPa ν ρ kg/m^3	210/110 0.305/0.28 7744/7100	180/210 0.3/0.3 8025/7200	–– –– ––
anisotropic	**II**/ – **IV**/ 31,355	E_{ij}GPa ν ρ kg/m^3	–/146 ––/0.29 ––/7100	see Table 3	207 7860

Table 3: An-isotropic lining material properties according to Figure 2 dependend on pressure [71] for model *IV*

Pressure MPa Material Constant	p_0 10^{-3}	p_1 0.5	p_2 2.5	p_3 5.0	p_4 8.0
E_{33}GPa	1.9	1.9	2.5	4.0	4.3
$E_{22} = E_{11}GPa$	12.8	12.8	13.0	13.1	13.2
$G_{12}GPa$	2.0	2.0	2.1	2.2	2.3
$G_{13} = G_{23}GPa$	4.0	4.0	4.2	4.4	4.6
$\nu_{23} = \nu_{13}$	0.51	0.51	0.41	0.32	0.30
$\nu_{32} = \nu_{31}$	0.08	0.08	0.105	0.11	0.115
$\nu_{12} = \nu_{21}$	0.08	0.08	0.105	0.11	0.115
ρkg/m^3	2500	2500	2500	2500	2500

The numerical simulations are performed using ABAQUS 6.8-4. The *Finite Sliding* formulation is chosen to model the contact with a kinematic constraint contact algorithm and a constant friction coefficient. In order to determine mesh-independent pad modes, a mesh study was undertaken [67]. The main findings of this mesh independence study are:

(1.) Convergence in unstable vibration modes predicted by the complex eigenvalue analysis (CEA) depends on the mesh resolution: if the mesh is too coarse, unstable modes might change easily with friction coefficients and/or too many modes might be predicted to be unstable (depending on the element type).

(2.) For pad modes, the mesh has to be significantly finer especially in the contact zone in order to obtain a converged solution. The mesh resolution is dependent on the elastic properties of the lining as well: Stiffer materials need to be meshed with a finer mesh than compliant lining.

(3.) Especially for a steel pad, due to variations in the mesh refinement resulting in small numerical stiffness changes, the mesh has to be even finer in the contact zone than for an anisotropic lining material. Here especially the in-plane stiffness seems to be important.

The meshs used here give a difference in the estimate of frequency of less than 1% when the number of elements is increased by around 298%. The number of elements and their type and the material properties for the four models are depicted in Table 2. Only *incompatible modes* elements (C3D8I) for improved bending behaviour are used [72]. The material properties of model IV are taken from Yuhas et al. [71] as shown in Table 2 for a pressure of 0.5MPa (M_1 in Figure 2). In Table 2, for models II and IV, only the reference material properties, are given.

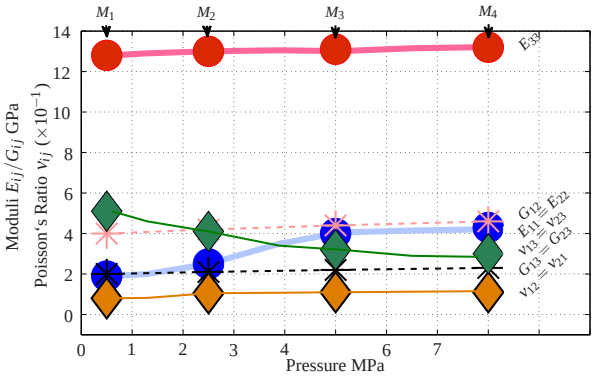

Figure 2: (color online) Material properties of measurements taken from Yuhas et al. [71]. The position of the markers (material points M_1 - M_4) indicate the values taken for a parameter study presented later in this chapter.

For the acoustic calculations, ESI's VAOne Fast Multipole Solver has been used, as recommended in [67]. Throughout this study, the speed of sound is set to $c = 340$m/s and the fluid's density to $\rho = 1.3$kg/m^3. For the acoustic power, the dB values greater than 68.51dB would be detected as squeal on a dynamometer test rig and performance tests, according to [73, 74], assuming a monopole source with a $\geq$ 70dB sound pressure level in a distance of 0.5m.

ACOUSTIC RADIATION OF FRICTION SYSTEMS

Isotropic Pad-on-plate (I)

The structural vibration of the pad-on-plate model I has been analysed using FEM in [65] whereas in here, the radiated acoustic power in the frequency range of 2.5 to 6.5kHz is plotted in Figure 3, for pressures from 10^{-3} to 8MPa and friction coefficients from 0.05 to 0.65. As reference, the acoustic power level for a potential squeal record is depicted by a horizontal dash-dotted line: Only, if the acoustic power level exceeds this limit, squeal would be recorded in the automotive industry according to the standard SAEJ2521 [73]. For comparison, the acoustic

power of the plate alone without the pad is depicted. It can be seen that only the plate mode at resonance f_1 peaks up.

The pad-on-plate model basically has two types of system modes: one type dominated by plate motion (e.g. f_1), and the other type dominated by pad motion (e.g. $f_2 - f_4$). With increasing pressure and an increasing friction coefficient, the acoustic power increases. Pad modes at resonances f_2 to f_4 show the strongest change in acoustic power with variation of μ compared to the resonance at f_1 when the friction coefficient is varied. This result shows that the instability previously studied by means of kinetic energy and non-linear times series analyses [65] is acoustically relevant. Further, the influence of pressure and friction coefficient on the acoustic power is very similar to that on the kinetic energy spectrum presented in [75].

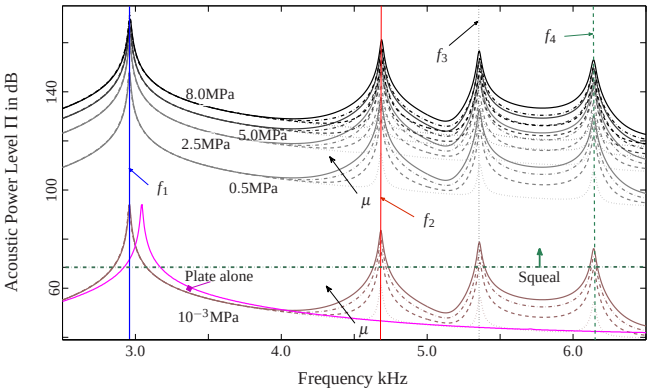

Figure 3: (colour online) Acoustic power over frequency for pressures $p_0 = 10^{-3}$MPa to $p_4 = 8.0$MPa over friction coefficients $\mu \in \{0.05, 0.25, 0.45, 0.65\}$

In Figure 4, the peak acoustic power for a (a) constant μ over a range of pressures p and a (b) constant p over a range of friction coefficients μ is depicted. Also, as a reference, the logarithm of the identity function and its square are plotted. From these reference functions, it is obvious, that similar relationships as for the kinetic energy [65] are found: for each friction coefficient, the effect of pressure on the acoustic power is more consistent than its effect due to varying friction coefficient at constant pressure. Especially for pressures above 1MPa this is obvious, and the relationship between pressure and acoustic power can be assumed to be more predictable than the relationship between the acoustic power and the friction coefficient and approximates the behaviour of a quadratic function. Further, it can be observed from 4 (a) that the acoustic power level in resonance f_1 decreases whereas the acoustic power level in f_3 increases

The radiation efficiency, σ, is the ratio of the radiated active power per unit area to the mechanical vibration power calculated from the vibration velocity distribution [76] which is also referred to as an infinite rigid baffle with the same surface area and an identical velocity distribution as the structure [77–79].

$$\sigma = \Pi / (\rho c S < \vec{v}^2 >) \qquad (1)$$

Here, Π corresponds to the radiated acoustic power, ρ is the fluid's density, c the speed of sound, S the surface area of the vibrating structure and $< \vec{v}^2 >$ is the spatial average of the mean square velocity response of the structure.

In Figure 5, the radiation efficiency for the isotropic pad-on-plate model (I) is depicted for pressures ranging from 0.001 MPa to 8.0MPa and friction coefficients from 0.05 to 0.65. The locations of resonances f_1 to f_4 are marked and for comparison, the radiation efficiency of only the plate is depicted as well

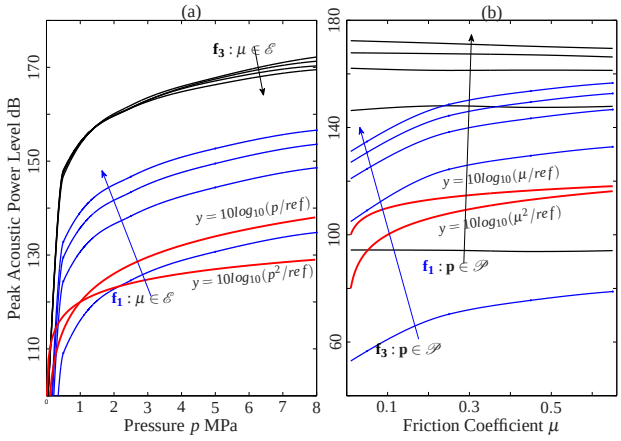

Figure 4: (colour online) Scattering of peak amplitudes of acoustic power exemplified by values taken at resonances f_1 and f_3 (figure 3) by varying (a) pressure or (b) friction coefficient, and by leaving either μ or p constant, respectively

and is generally higher than that of the pad-on-plate system. However, without the contact, the plate alone would not squeal therefore the plate alone marks only a reference whithout being actually relevant for brake squeal. Anyway, it is interesting to note that between 5.5 and 5.8kHz, the radiation efficiency of the pad-on-plate model is higher than the plate's. In this region of higher σ, the friction coefficient produces large changes but for a given friction coefficient, pressure has no effect on the radiation efficiency, as shown in Figure 5 as the curves of σ for different pressures lie on top of each other for each μ. Secondly, the radiation efficiency for a friction coefficient of $\mu = 0.05$ has shows minima at location of resonances $f_2 - f_4$. However, these minima change with increasing μ: f_2 does not show an extremum which can be associated with the former minimum any more, the minimum at f_3 moves from 5.4 to 5.2kHz and the minimum at f_4 moves from 6.15 to 6.4kHz. The global minimum in radiation efficiency occurs at around 5.2kHz and the maximum around 5.7 kHz (between f_3 and f_4). This means that it would be quite efficient to initiate squeal at around $5.45 - 5.96\text{kHz} \approx [f_3, f_4]$. On the other hand, around $4.5 - 5.3\text{kHz} \approx [f_2, f_3]$, relatively high vibration amplitudes are required to generate squeal. It is interesting to note that the squeal frequency at around 5.7kHz reported in [12] is also at this frequency, which is where the radiation efficiency has its maximum.

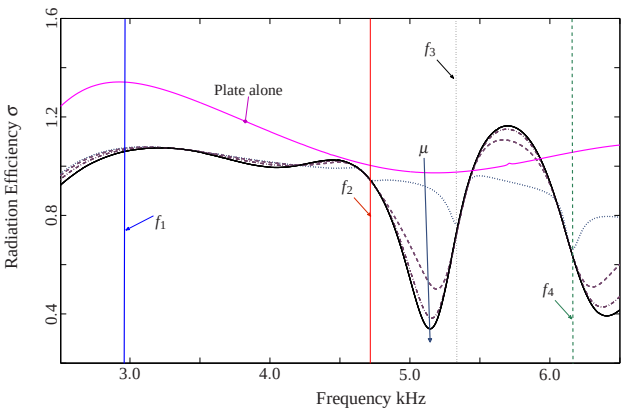

Figure 5: Radiation efficiency for pressures p_0 to p_4 over friction coefficients $\mu \in \{0.05, 0.25, 0.45, 0.65\}$

Next, the dependency of the radiation efficiency on pressure and friction coefficient is investigated. The dependency of the radiation efficiency on varying pressure relative to $p_0 = 1$kPa for a constant μ is depicted in Figure 6 and expressed in terms of $\Delta\sigma|_{\mu=const.} = (1 - \sigma_{p_i}/\sigma_{p_0}) \times 100$ for $i \in \{1,...,4\}$: all radiation efficiencies are relative to the radiation efficiency at a pressure of 1kPa. As can be seen, at resonances f_3 and f_4, the deviations due to pressure variations are the highest but never exceed 1%. For a small μ, the change due to pressure variations is smaller than for the higher μ. This means that if $\Delta\sigma$ becomes negative, in the case of increasing pressure at high μ, the acoustic power increases stronger than does the strength of the underlying velocity field and vice versa. The extrema of relative changes due to pressure variations fall almost together with resonances f_3 (minimum) and f_4 (maximum) (Figure 6).

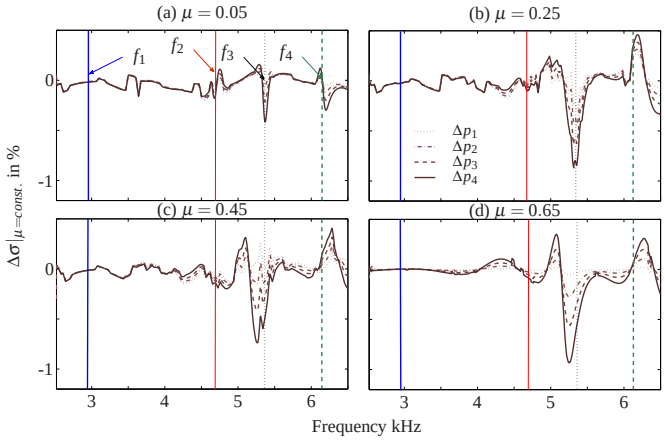

Figure 6: Relative change of radiation efficiency for pad-on-plate model (I) with variation in pressure and varying pressure

In Figure 7, the dependency of the radiation efficiency on friction coefficients for constant pressure is analysed. For each curve, μ was varied for one selected pressure and set into ratio to the radiation efficiency at $p_0 = 1$kPa and μ ($\Delta\sigma|_\mu$). Clearly, the friction coefficient has a much stronger influence than pressure, and relative changes of up to 70% can be observed, especially in the intervals $[f_2, f_3]$ and $[f_4, 6.5]$kHz. Qualitatively, not many changes in Figure 7 can be observed. The only remarkable change is around 4, 5 or 6.4kHz where, the percentage of radiation efficiency ratios due to changed friction coefficients increases. Local Minima of $\Delta\sigma|_\mu$ fall together with resonances and with increasing pressure these minima are slightly more pronounced.

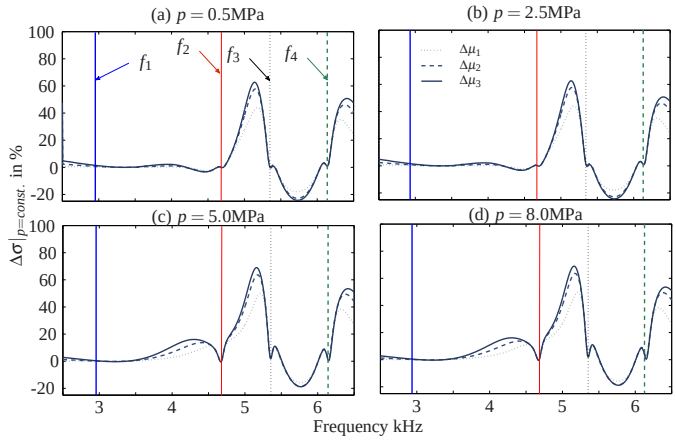

Figure 7: Radiation efficiency: changes with variations of friction coefficient and constant pressure

It can be concluded that varying the pressure does not significantly change the radiation characteristic of the pad-on-plate system. In contrast, a variation of the friction coefficient may alter the acoustic efficiency significantly at some frequencies. If only mode coupling is considered with no pad-modes in the frequency range considered, a robust (in the sense of NVH needs) design of a brake system should aim at a sufficiently large frequency spacing and at reducing σ in critical regions.

Isotropic Pad-on-disc (III)

Figure 8(a) depicts the acoustic power and (b) the radiation efficiency of model III. The numbering of the dominant resonances f_1 to f_{15} is applied in accordance with the kinetic energy spectrum analysed in [65]. Compared with the kinetic energy spectrum studied in [65], the acoustic power spectrum looks very similar for isotropic pad-on-disc system. However, one important and obvious difference is shown: the isotropic pad-on-disc system cannot squeal at the disc's in-plane shear mode ($l = 0$) at resonance at f_4 (Figure 8(a)). Similar to pad modes P_r, P_t and P_{rot}, this mode is an in-plane mode which exhibits a large amount of fed-in energy but is not predicted to be unstable by the complex eigenvalue analysis [65].

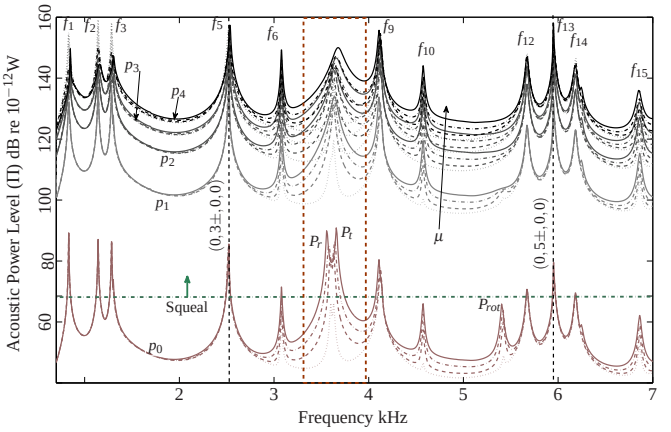

(a) Acoustic Power

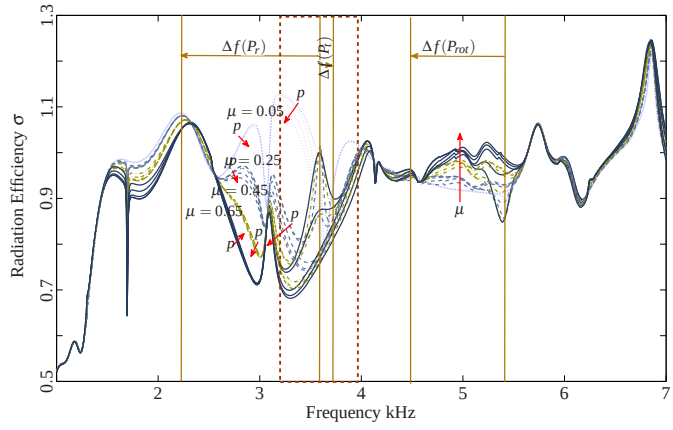

(b) Radiation Efficiency

Figure 8: (a) Acoustic power level (Π) and (b) radiation efficiency (σ) for isotropic pad-on-disc system with (I) synchronised pressure-(p) and friction coefficient (μ) variations

From structural vibration analysis alone, by looking at the results of a CEA or the global kinetic energy spectrum only, it is not possible to predict which of these in-plane modes is acoustically relevant. Further, by calculating the radiated acoustic power, it can be seen from Figure 8(a), that the isotropic steel pad-on-disc already produces squeal at very low pressure values as the acoustic power in some peaks exceeds 68.51dB. In

Figure 8 (b), again the radiation efficiency for various pressures and friction coefficients is depicted. However, the changes due to pressure variations are here more obvious than for the pad-on-plate system (Figure 5). For the isotropic pad-on-disc system, the three regions of the radial, tangential and rotational mode seem especially important, which are marked by horizontal arrows within the interval boundaries (P_r, P_{rot}) and by a dashed box (P_t). The intervals were assigned to the span of frequency variation prior to a complex eigenvalue extraction step [65]. For the radial pad mode, the interval is $[2.2, 3.6]$ kHz and P_{rot} it is the interval from $[4.5, 5.4]$ kHz. Again, as in the case of the pad-on-plate system, changes due to μ variations are stronger than those for variations in p. Marked by arrows is the development of σ with changing p or μ. Here, the interval of $P_{rot} \in [4.5, 5.4]$ kHz is easier to interpret as, for this mode, the resonance f_4 in the acoustic power spectrum (Figure 8(a)) vanishes after a pressure of $p_1 = 0.5$MPa, and the increase in σ for increases in p and μ must be due to a decreasing value of the surface velocity distribution. More difficult is the interpretation of the other two intervals assigned to P_r and P_t. Here, in general, the radiation efficiency decreases with increasing μ and p which indicates that the velocity increases faster than the radiated acoustic power. This is especially true for the unstable $n = 3$ mode at f_5 predicted by CEA and for the stable mode at f_6. The radial and tangential pad modes P_r and P_{rot} (dashed square) show high radiation efficiencies at low pressures and high friction coefficients, or at low friction coefficients only. This confirms the assumption that these modes, if present in the acoustic power spectrum, are prone to squeal in the low-pressure regime at low friction coefficients with only a small surface normal velocity necessary to initiate squeal. For pressures greater than 0.5MPa, the radial pad mode is no longer visible in the acoustic power spectrum, but its effects are still perceivable in the radiation efficiency, as shown in Figure 8(b). Also, the $\Delta\sigma|_\mu$ is up to 20% higher than that of the pad-on-plate system, which suggests that for model III variations in pressure being more important than for the pad-on-plate model I. In Figure 9 (a), changes in radiation efficiency, relative to a pressure of $p_0 = 0.001$kPa for a constant μ, are depicted. Changes, of up to 20%, can be observed around pad modes P_r, P_t and P_{rot}. The differences relative to the values of the reference pressure increase for both increasing pressure and increasing friction coefficient. Again, changes in the radiation efficiency are mainly due to variations in μ. The contributions due to pressure changes are smaller (Figure 9 (b)) which is similar to observations in the pad-on-plate model I (Figure 6 and 7). However, the difference between $\Delta\sigma|_\mu$ and $\Delta\sigma|_p$ decreases (of now only a maximum span difference of 17%), indicating, that the pressure becomes more important. Also, as for model I, at resonances, the change of the radiation efficiency due to pressure is highest if the friction coefficient remains constant. In Figure 9 (b), only changes relative to a friction coefficient of $\mu = 0.05$ for a pressure of 8MPa are depicted as, in comparison with other pressures, no significant differences are observed. For the isotropic pad-on-disc it can be stated as well that from the analysis of the radiation efficiency the main contributing factor to changes in the radiation efficiency lies in the variation of the friction coefficient. Further, it is interesting that minima of radiation efficiency mostly lie closeby resonance frequencies and that only the disc's in-plane shear mode $l = 0$ gives an exposed peak and an increase in radiation efficiency with increasing friction coefficient. The sidebands of resonance f_6 and P_r, P_t show the highest positive change to friction coefficient variations, indicating high squeal propensity here prior to μ increases.

Case Study (Model III)

Next, for the isotropic pad-on-disc model, the acoustic power is calculated at frequencies of all vibration modes calculated by the complex eigenvalue method in the frequency range of $1-7$kHz for friction coefficients from 0.05 to 0.65. Calculations

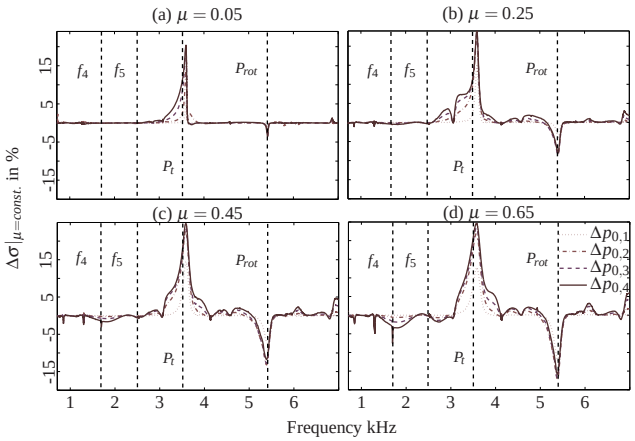

(a) Constant friction coefficient, $\Delta\sigma|_{\mu=const.}$

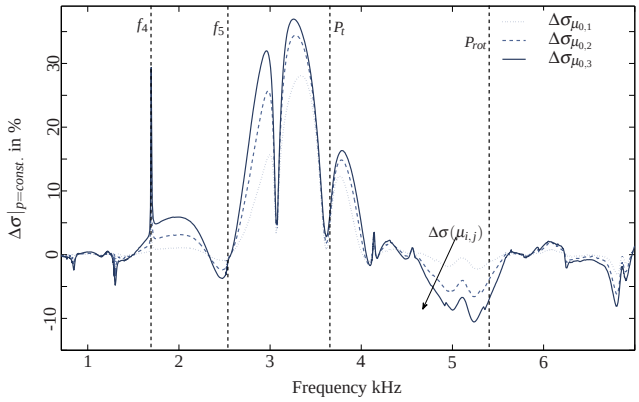

(b) Constant pressure 8MPa, $\Delta\sigma|_{p=const.}$

Figure 9: Sensitivity of the isotropic pad-on-disc model (III) to changes in (a) pressure with constant friction coefficient and (b) friction coefficient with constant pressure of $p = 8.0$MPa

are performed at only selected frequencies of interest rather than over a whole frequency range which greatly reduces the computational time required. The pressure is kept at a low value of 1kPa. The use of frequencies extracted by means of a complex eigenvalue analysis step gives a little fuzziness as the in-vacuo modes do not represent the globally damped system's response due to excitation [65] which can influence the exact frequency and, hence, the vibration response at resonance. However, the deviation of the frequency of unstable modes determined by CEA from the resonance peak in the forced response is, on average, below 1.2%. The three cases studied are listed below.

(A) undamped system modes, pad constrained with first and last 10% of nodes (stiffened boundary condition, see [67]); $n = 4$ and $n = 5$ split modes become unstable;
(B) case A but with global structural damping of $\zeta = 0.4\%$; $n = 4$ and $n = 5$ split modes become unstable; and
(C) compliant boundary condition with global structural damping $\zeta = 0.4\%$; $n = 3$ and $n = 5$ split modes unstable.

For the system with stiffened BC the pad modes, as for those in the isotropic pad-on-plate model (I), do not fall in the frequency range of $1-7$kHz.

Case A In Figure 10, the undamped stiff system of case A is investigated. In total, 18 modes are extracted but only the most prominent modes are plotted in thicker lines and marked by arrows. All other modes, are plotted in dotted lines. The two transition points, which are the points where the split modes merge, are denoted by TP_1 and TP_2. The transition point consists at the x axis of the critical friction coefficient and on the $y-$axis of the acoustic power, the two coupled modes radiate.

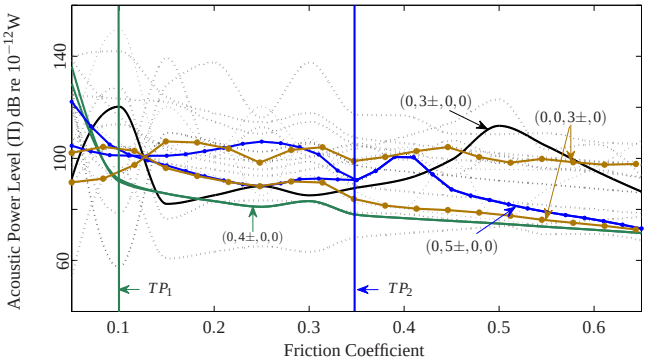

Figure 10: Case A: undamped isotropic pad-on-disc system (III) with stiffened boundary conditions- pad modes *absent* in frequency range investigated

As in the model at hand, only split modes merge, which have the same modeshape, it is expected, that the radiated acoustic power is the same for both modes if they coupled and radiate at the same frequency. In Figure 11 clearly, after the modes merge, the radiated acoustic powers of the two split modes are identical, indicating that they vibrate at the same frequency. However, for most friction coefficient values, other modes such as the $q = 3$ in-plane mode (star mode), radiate more acoustic power than the unstable out-of-plane modes.

Case B In Figure 11, the acoustic power of the damped pad-on-disc model (III) is depicted. Evidently, the overall level of acoustic power is reduced and most of the modes no longer oscillate with increasing friction coefficient. For the complex eigenvalue analysis it is known and suggested in [80] to incorporate frictional damping by applying a friction law with a negative slope of the friction coefficient due to increasing relative velocity: By doing this, many modes, being previously predicted to be unstable are damped out and the prediction quality is enhanced. This effect of damping is here also encountered but by applying global structural damping. The unstable $n = 4$ mode radiates maximum acoustic power at $\mu = 0.4$ even though the critical coefficient of friction is at a $\mu = 0.15$. A mode-merging in terms of acoustic power is no longer clearly visible at exactly the transition points TP_1 and TP_2. The same holds true for the $n = 5$ mode where the critical friction coefficient is determined by the complex eigenvalue method to be 0.35 but the acoustic power for the positive and negative travelling waves is equal only at $\mu = 0.41$ which is an effect of system behaviour, due to the participation of other modes and structural damping, both absent for the CEA. In addition, previous findings in [43, 44] show that the critical friction coefficient does not necessarily indicate whether the system starts squealing. This is confirmed here by the unstable modes $n = 4$ and $n = 5$, for which the maximum acoustic power occurs at friction coefficients different from μ_{crit} at TP. This means that either squeal starts at the maximum or that the increase in acoustic power and the difference between the value found at the transition point and its maximum value would represent a potential of increasing acoustic power amplitude in the time domain. Generally in a first approximation it is assumed, that at

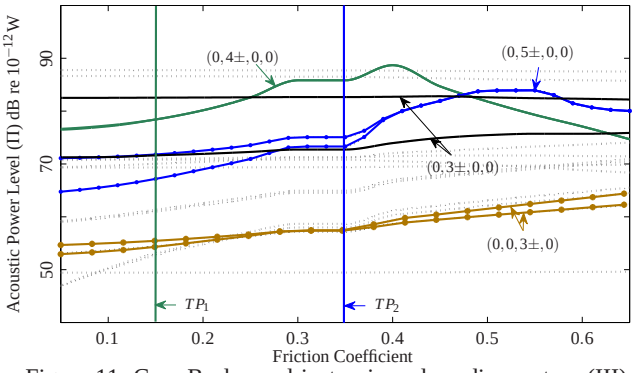

Figure 11: Case B: damped isotropic pad-on-disc system (III) with stiffened boundary conditions - pad modes *absent* in frequency range investigated

higher speeds (lower friction coefficients), the system behaves stable. By increasing the friction coefficient, a quasi-time dependent analysis in the frequency domain is performed, as it is assumed, that in the course of the braking process, the vehicle is slowed down and as such also the relative velocity between pad and disc decreases, leading to higher friction.

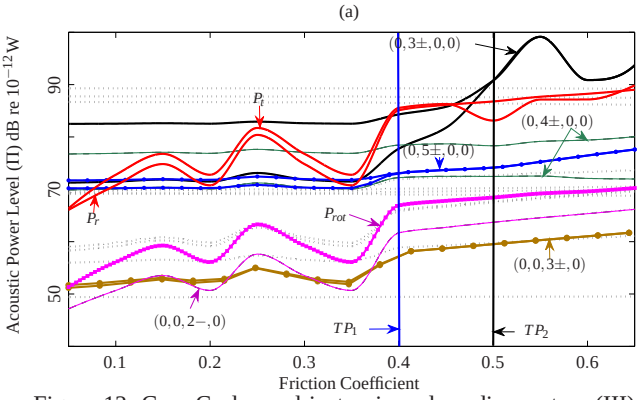

Figure 12: Case C: damped isotropic pad-on-disc system (III) with compliant boundary conditions- pad modes *present* in frequency range investigated

Case C The acoustic power for the 21 modes of case C is depicted in Figure 12. The system is more compliant and the pad modes previously found above 7kHz now occur at around 3.8kHz [67]. They are denoted by P_r, P_t and P_{rot}, in accordance with [65], and stand for radial, tangential and rotational pad modes, respectively. The $n = 3$ and $n = 5$ modes are predicted to be unstable. The acoustic power of the pad modes exhibits oscillatory behaviour with increasing friction coefficient. Modes close to the pad-mode frequencies such as the $(0,0,2-,0)$ or $(0,0,3,0)$-mode, seem to be influenced by these oscillations. These oscillations have been observed in contour plots of acoustic power over the frequency and friction coefficients in Oberst and Lai [44]. This highlights the effects of the friction coefficient on the acoustic power radiation of pad modes, causing them to fluctuate with a trend towards higher values [65].

In this case study, it is shown that: (1) global damping is necessary in order to isolate unstable modes predicted by the complex eigenvalue method and to damp out oscillations in acoustic power; (2) the radiated acoustic power of pad modes oscillate with the friction coefficient and influence the neighbouring modes like the radial in-plane disc modes $(0,0,2-,0)$ and $(0,0,3,0)$, so that their acoustic power also oscillates ; and (3) the maximum of acoustic power does not occur at critical fric-

tion coefficient but shortly after the critical coefficient or the transition point, which might represent a potential of increase in acoustic power level.

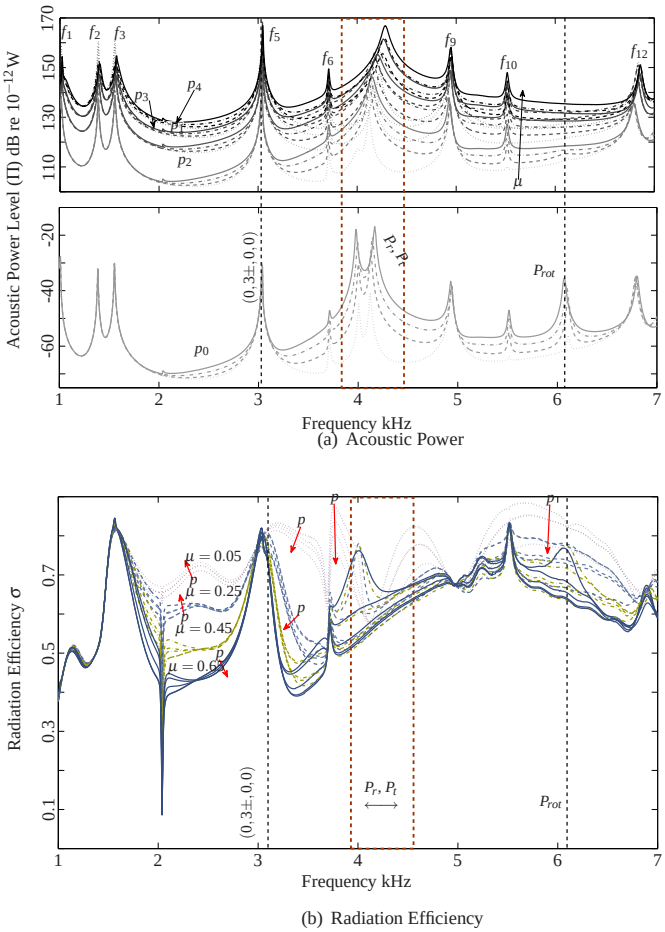

Figure 13: Acoustic power and radiation efficiency for anisotropic pad-on-disc model (IV) with synchronised pressure and friction coefficient variations

Anisotropic Pad-on-Disc (IV)

Figure 13(a) depicts the acoustic power spectrum for different pressures, with a range of friction coefficients at each pressure. Similar to the kinetic energy spectrum in [65], the radiated acoustic power increases with increasing pressure or friction coefficient. The increase in acoustic power at resonances of pad modes P_t and P_{rot} due to increases in the friction coefficient is significantly higher than for modes associated with other resonances. Also interesting is the vanishing of P_r and P_{rot} after the pressure is increased to $p_1 = 0.5$MPa. Although the main movement of the three pad modes is in-plane, these modes are acoustically relevant because the disc vibration at this frequency has an out-of-plane component which is vibrationally active. However, at very low pressures such as $p_0 = 0.001$MPa, the acoustic power is very small, less than 68.52dB, which means that in 0.5m distance the brake noise recorded would be below a sound pressure level (SPL) of 70dB and hence not counted as squeal [74]. It is not clear at which exact pressure between $p_0 = 0.001$MPa and $p_1 = 0.5$MPa the pad-on-disc system is able to produce noise above SPL=70dB. In Figure 13 (b), the spectrum of radiation efficiency is depicted for variations in friction coefficient and pressure. Below 1.8kHz, the radiation efficiency is largely unchanged. Above 1.8kHz, σ increases with increasing pressure, but again the friction coefficient has a much stronger effect on σ especially at $2-3$kHz. Above 3kHz the σ mainly decreases with increasing pressure and μ. Pad modes P_r and P_t only have higher values of σ for low friction coefficients or, in the case of $p_0 = 0.001$MPa, where P_r is still identifiable in the acoustic power spectrum of Figure 13 (a). Although the acoustic power increases with μ, the velocity distribution becomes far stronger so that the radiation efficiency decreases, thereby indicating higher squeal propensity at the beginning of a brake stop. The radiation efficiency of the unstable mode $(0, 3+, 0, 0)$, at a squeal frequency around 3kHz, is almost unaffected by pressure or friction coefficient. For frequencies above 5kHz, the radiation efficiency of the rotational pad mode P_{rot} at a friction coefficient of $\mu = 0.65$ and p_0.

Figure 14 displays the change of the radiation efficiency due to (a) pressure and (b) friction coefficient variations relative to the reference values of $p_0 = 0.001$MPa and $\mu = 0.05$, respectively. In Figure 14 (a), differences in the radiation efficiency up to 20% are obtained indicating the importance of prescribing pressure in the calculations of acoustic radiation. In the neighbourhood of P_r, P_t and P_{rot}, the radiation efficiency changes significantly their maxima are no longer as clearly aligned with the resonances of the acoustic power spectrum as it was the case for the isotropic pad-on-disc system (Figure 9 (a)). In Figure 14(b), changes in σ due to variations in μ indicate that, friction coefficient variations are most influential.

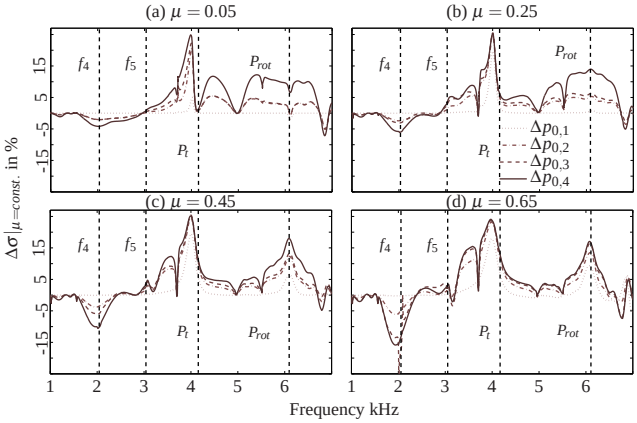

(a) Constant friction coefficient, $\Delta\sigma|_{\mu=const.}$

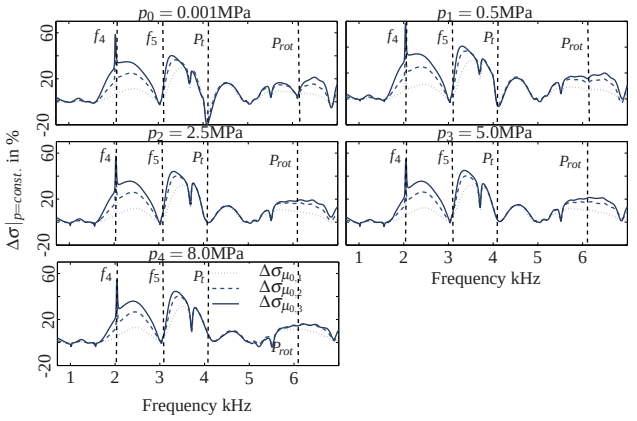

(b) Constant pressure 8MPa, $\Delta\sigma|_{p=const.}$

Figure 14: Anisotropic pad-on-disc's model (IV) changes in radiation efficiency to variations in (a) pressure with constant friction coefficient and (b) friction coefficient with constant pressure

CONCLUSIONS

It has been shown in this paper that vibrations initiated by pad-modes vibrations are also acoustically relevant for pad-on-disc systems such as models III and IV. For the steel lining material (model III) or the more realistic lining material of model IV, pad modes investigated radiate efficient at low pressures and lower friction coefficients as can be seen from plots of radiation efficiency. However, for model IV, as the acoustic power is relatively low at $p_0 = 1$kPa, squeal might not occur. Its transition to audible squeal lies somewhere in the region between 1kPa and 0.5MPa. In contrast to model IV, for the isotropic pad-on-disc model, even very low pressures lead to squeal, as the acoustic power is much higher at for instance 1kPa. This confirms assumptions in [81, 65] and highlights the differences and similarities between beam-on-disc setups and real brake systems.

It can be concluded, that (1) squeal propensity is higher at lower pressures, (2) radial and rotational pad modes P_r and P_{rot} are an additional source of instability and might lead to squeal with high sound power and high radiation efficiency for model IV in the interval of $]0.001, 0.5\text{MPa}]$ for model III even at 1kPa, and (3) kinetic energy for the tangential pad mode is not consumed by other squeal mechanisms as is the case for the in-plane $l = 0$ shear mode. For higher pressures, as the acoustic power is not attenuated, it can be assumed that squeal is still an issue at the frequency of P_t but that, simultaneously, more energy is either dissipated or fed in, as expressed by lower radiation efficiencies, prior to higher mean squared velocities.

Further, it has been found that the friction coefficient has a much stronger influence on the radiation efficiency than pressure for all three models I, III and IV. Pressure is more important for the two pad-on-disc models III/IV. A higher non-linearity and less consistent behaviour of the fed-in energy is found for varying the friction coefficient than for varying the pressure: changes in acoustic power due to increasing pressure can be approximated by a squared function. This statement cannot be given for a variation in friction coefficient, as peak acoustic power levels change without a clear tendency (Figure 4). This behaviour was also found for the pad-on-disc models, but for the sake of brevity not depicted here, as it is only slightly different from the development of peak kinetic energy changes studied in [65]. The pad modes, as they are in-plane acting, are responsible for the load of the fed-in energy; this can either lead directly to squeal in the sense of a pad-mode instability by activating the underlying out-of-plane disc vibrations or transfer the energy to a mode-coupling instability very similar to parametric resonances described in [82, 20]. It has been shown that unstable pad modes contribute to squeal by amplifying the out-of-plane disc vibrations or transferring energy to a mode-coupling instability. Also, P_r act radially and are hence very similar to the transient mechanism found by Kindaid et al.[58] which is responsible for squeal at low pressures.

It is difficult to predict squeal frequencies by complex eigenvalue analysis or structural in-plane vibrations obtained by a forced response because, although they might be vibrationally unstable, they might not be acoustically relevant, as shown by resonance f_4 and the pad modes. All modes at resonances f_4, P_r, P_t and P_{rot} are inplane modes, but only the tangential pad mode remains acoustically relevant over a range of pressures and friction coefficients . Although the in-plane $n = 0$ shear mode, $l = 0$, is vibrationally very active and feeds in a lot of energy into the system, it does not show any peak in the acoustic response. Results here show that in addition to performing a complex eigenvalue analysis or an analysis of feed-in energy, additionally calculations of kinetic energy and acoustic power levels should be performed as mechanisms for squeal other than mode-coupling can be subsequently isolated and treated in design modifications.

ACKNOWLEDGEMENTS

This research was undertaken on the NCI National Facility in Canberra, Australia, which is supported by the Australian Commonwealth Government. The first author acknowledges receipt of a University College Postgraduate Research Scholarship for the pursuit of this study and the Australian Acoustical Society for a *Young Scientist's Award* to participate at the ICA2010 Conference.

REFERENCES

[1] S. Oberst and J. Lai. A critical review on brake squeal and its treatment in practice. In *Internoise 2008, Shanghai*, 2008.

[2] H. Abendroth and B. Wernitz. The integrated test concept: Dyno-vehicle, performance-noise. *SAE Technical Paper Series*, 2000-01-2774, 2000.

[3] D. Stanef, A. Papinniemi, and J. Zhao. From protoype to production - the practical nature of brake squeal noise. *SAE Technical Paper Series*, 2006-01-3217:1–10, 2006.

[4] A. Akay. Acoustics of friction. *Journal of the Acoustical Society of America*, 111(4):1525–1548, 2002.

[5] A. Papinniemi, J. Lai, J. Zhao, and L. Loader. Brake squeal: a literature review. *Applied Acoustics*, 63:391–400, 2002.

[6] N.M. Kinkaid, O.M. O'Reilly, and P. Papadopoulos. Automotive disc brake squeal. *Journal of Sound and Vibration*, 267:105Ű166, 2003.

[7] F. Chen, F. Tan, C./Chen, C. A. Tan, and R. L. Quaglia. *Disc Brake Squeal: Mechanism, Analysis, Evaluation and Reduction/Prevention*. SAE-Society of Automotive Engineers, 2006.

[8] H. Ouyang, W. Nack, Y. Yuan, and F. Chen. Numerical analysis of automotive disc brake squeal: a review. *International Journal of Vehicle Noise and Vibration*, 1:207–231, 2005.

[9] N. Hoffmann and L. Gaul. Friction induced vibrations of brakes: Research fields and activities. *SAE Technical Paper Series*, 2008-01-2579:1–8, 2008.

[10] V.P. Sergienko, S. N. Bukharov, and A. V. Kupreev. Noise and vibration in brake systems of vehicles. part 1: Experimental procedures. *Journal of Friction and Wear*, 29(3):234–241, 2008.

[11] V.P. Sergienko and S. N. Bukharov. Vibration and noise in brake systems of vehicles. part 2: Theoretical investigation techniques. *Journal of Friction and Wear*, 30:216–226, 2009.

[12] F. Chen. Automotive disk brake squeal: an overview. *International Journal of Vehicle Design*, 51(1/2):39–72, 2009.

[13] F. P. Bowden and L. Leben. Nature of sliding and the analysis of friction. *Nature*, 3572:691–692, 1938.

[14] F. P. Bowden and D. Tabor. Mechanism of metallic friction. *Nature*, 3798:197–199, 1942.

[15] C.M. Mate, G.M. McClelland, R. Erlandsson, and S. Chiang. Atomic-scale friction of a tungsten tip on a graphite surface. *Phys. Rev. Lett.*, 59:1942–1945, 1987.

[16] H.R. Mills. Brake squeak. Technical report, The Institution of Automobile Engineers, Research Report, 9000 B and 9162 B, 1938.

[17] R.T. Spurr. A theory of brake squeal. *Proceedings of the Automobile Division, Institution of Mechanical Engineers 1961-1962 (1)*, 1:33–52, 1961.

[18] M.R. North. Disc brake squeal - a theoretical modell. Technical Report 5, Motor Industry Research Association, Warwickshire, England, 1972.

[19] S.K. Rhee, P.H.S. Tsang, and Y.S. Wang. Friction-induced noise and vibration of disc brakes. *Wear*, 133:39–45, 1989.

[20] J.E. Mottershead, H. Ouyang, M.P. Cartmell, and M.I. Friswell. Parametric resonances in an annular disc with a rotating system of distributed mass and elasticity: And the effects of friction and damping. *Proceedings: Mathematical, Physical and Engineering Sciences*, 453(1956):1–19, 1997.

[21] H. Ouyang, J.E. Mottershead, M.P. Cartmell, and M.I. Friswell. Friction-induced parametric resonances in discs: effect of a negative friction-velocity relationship. *Journal of Sound and Vibration*, 209(2):251–264, 1998.

[22] H. Ouyang. Moving loads and car disc brake squeal. *Noise & Vibration WORLDWIDE*, 34(11):7–15, December 2003.

[23] J.R. Barber. The influence of thermal expansion on the friction and wear process. *Wear*, 10(2):155 – 159, 1967.

[24] J.R. Barber. Thermoelastic instabilities in the sliding of conforming bodies. *Royal Society of London Proceedings Series A Mathematics Physics and Engineering Science*, 312(1510):381 – 394, 1969.

[25] N. Hoffmann and L. Gaul. Effects of damping on mode-coupling instability in friction induced oscillations. *ZAMM, Z. Angew. Math. Mech.*, 83(8):524–534, 2003.

[26] G.G. Adams. Self-excited oscillations of two elastic half-spaces sliding with a constant coefficient of friction. *ASME Journal of Applied Mechanics*, 62:867–872, 1995.

[27] G.G. Adams. Steady sliding of two elastic half-spaces with friction reduction due to interface stick-slip. *ASME Journal of Applied Mechanics*, 65:470–475, 1998.

[28] V. Linck, L. Baillet, and Y. Berthier. Modelling the consequences of local kinematics of the first body on friction and on the third body sources in wear. *Wear*, 255:299–308, 2003.

[29] A.S. Merriweather. Acoustic radiation impedance of a rigid annular ring vibrating in an infinite rigid baffle. *Jounal of Sound and Vibration*, 10(3):369–379, 1969.

[30] M. Sathyamoorthy. Nonlinear vibrations of plates. a review. *Shock & Vibration Digest*, 3-16(6):13pp, June 1983.

[31] M. C. Junger and D. Feit. *Sound, structures, and their interaction (2nd edition)*. Cambridge, MA, MIT Press, 1986, 460 p., 1986.

[32] I.Y. Shen and C.D. Mote Jr. On the mechanisms of instability of a circular plate under a rotating spring-mass-dashpot system. *Jounal of Sound and Vibration*, 148(2):307–318, 1991.

[33] K. M. Liew, Y. Xiang, and S. Kitipornchai. Research on thick plate vibration: a literature survey. *Journal of Sound and Vibration*, 180(1):163–176, February 1995.

[34] F. Zhang, L. Cheng, L.H. Yam, and L.M. Zhou. Modal characteristics of a simplified brake rotor mode using semi-analytical rayleigh-ritz method. *Jounal of Sound and Vibration*, 297:72–88, 2006.

[35] H. Lee and R. Singh. Acoustic radiation from out-of-plane modes of an annular disk using thin and thick plate theories. *Journal of Sound and Vibration*, 282(1-2):313–339, April 2005.

[36] I.Y. Shen. Vibration of rotationally periodic structures. *Jounal of Sound and Vibration*, 172(4):459–470, 1994.

[37] A. Cote, N. Atalla, and J.-L. Guyader. Vibroacoustic analysis of an unbaffled rotating disk. *Journal of the Acoustical Society of America*, 103(3):1483–1492, 1998.

[38] D.J. Ewins. *Modal Testing: theory, practice and application*. Research Studies Press, 2000.

[39] H. Lee and R. Singh. Self and mutual radiation from flexural and radial modes of a thick annular disc. *Journal of Sound and Vibration*, 286:1032–1040, 2005.

[40] F. Selimefendigil. Sound propagation behaviour of brake discs using numerical techniques. Master's thesis, Technische Universität München, 2006.

[41] B. L. Stoimenov, K. Adachi, and K. Kato. Analysis of frictional sound using radiation efficiency. In *9th Int. Congress on Sound and Vibration, Orlando, Florida, USA*, 2002.

[42] B. L. Stoimenov and K. Kato. The relationship between frictional sound and lumps build-up at the contact interface in single-pass dry sliding between aluminium pin and flat. In *Transient Processes in Tribology*, 2004.

[43] S. Oberst and J.C.S. Lai. Acoustic response of a simplified brake system by means of the boundary element method. In *NOVEM2009, Keble College, Oxford, England, 5-8April*, 2009.

[44] S. Oberst and J.C.S. Lai. Numerical prediction of brake squeal propensity using acoustic power calculation. In *Proceedings of ACOUSTICS 2009*, 2009.

[45] T. Irie, G. Yamada, and S. Aomura. Free vibration of a mindlin annular plate of varying thickness. *Journal of Sound and Vibration*, 66(2):187–197, 1979.

[46] T. Irie, G. Yamada, and K. Takagi. Natural frequencies of thick annular plates. *Journal of Applied Mechanics*, 49:633–638, 1982.

[47] W.P. Rdzanek Jr and Z. Engel. Asymptotic formulas for the acoustic power output of a clamped annular plate. *Applied Acoustics*, 60:29–43, 2000.

[48] W.P. Rdzanek Jr. The energy aspect of the reciprocal interactions of pairs of two different vibration mode of a clamped annular disc. *Journal of Sound and Vibration*, 249:207–323, 2002.

[49] W.P. Rdzanek Jr, W.J. Rdzanek, and Z. Engel. Theoretical analysis of sound radiation of an elastically supported circular plate. *Jounal of Sound and Vibration*, 265:155–174, 2003.

[50] W.P. Rdzanek Jr. The sound power of an individual mode of a clamped-free annular plate. *Jounal of Sound and Vibration*, 261:775–790, 2003.

[51] M. Lee and R. Singh. Analytical formulations for annular disk sound radiation using structural modes. *Journal of Acoustical Society of America*, 95(6):3311–3323, June 1994.

[52] O. Beslin and J. Nicolas. Modal radiation from an unbaffled rotating disk. *Journal of the Acoustical Society of America*, 100:3192–3202, 1996.

[53] A. Cote. Résponse vibratoire et acoustique d'un disque annulaire non-bafflé en rotation. Master's thesis, Sherbrooke University, Sherbrooke, Québec, Canada, 1994.

[54] H. Lee and R. Singh. Vibro-acoustics of a brake rotor with focus on squeal noise. In *Internoise 2002, Dearborn, MI, USA*, 2002.

[55] H. Lee. *Modal Acoustic Radiation Characteristics of a Thick Annular Disk*. PhD thesis, Graduate School of The Ohio State University, 2003.

[56] H. Lee and R. Singh. Determiniation of sound radiation from a simplified disc-brake rotor by a semi-analytical method. *Noise Control Engineering Journal*, 52(5):225–239, Sept-Oct 2004.

[57] N.M. Kinkaid. *On the Nonlinear Dynamics of Disc Brake Squeal*. PhD thesis, University of California at Berkeley, 2004.

[58] N.M. Kinkaid, O.M. O'Reilly, and P. Papadopoulos. On the transient dynamics of a multi-degree-of-freedom friction oscillator: a new mechanism for disc brake noise. *Journal of Sound and Vibration*, 287:901–917, 2005.

[59] E. Loesche. Energiegrößen basierte Beitragsanalyse beim akustischen Außenraumproblem. Master's thesis, Fakultät Maschinenwesen, Institut für Festkörpermechanik, 2009.

[60] S. Oberst and J.C.S. Lai. Numerical analysis of a simpli-

fied brake system. In *NOVEM2009, Keble College, Oxford, England,5-8April*, 2009.

[61] S. Oberst and J.C.S. Lai. Non-linear analysis of brake squeal. In *ICSV16, Krakow, 5-9 July*, 2009.

[62] J. Flint and J. Hald. Traveling waves in squealing disc brakes measured with acoustic holography. *SEA Technical Papers*, 2003-01-3319:1–8, 2003.

[63] J. C. Bea and J. A. Wickert. Free vibration of coupled disc-hat structures. *Journal of Sound and Vibration*, 235(1):117–132, 2000.

[64] M.J.K. Patching. Vibro-acoustic studies of brake squeal noise. Master's thesis, School of Aerospace, Civil and Mechanical Engineering, University College, University of New South Wales, Australian Defence Force Academy, 2003.

[65] S Oberst and J.C.S. Lai. Numerical study of friction-induced pad mode instability in brake squeal. In *20th International Congress on Acoustics (ICA 2010) in Sydney, 23 - 27 August, Australia*, 2010.

[66] R.A. AbuBaker and H. Ouyang. A prediction methodology of disk brake squeal using complex eigenvalue analysis. *Int. J. Vehicle Design*, 46:416–435, 2008.

[67] S Oberst and J.C.S. Lai. Methodology of numerically simulating brake squeal noise by means of a simplified brake system. In *20th International Congress on Acoustics (ICA 2010) in Sydney, 23 - 27 August, Australia*, 2010.

[68] N. Hinrichs, M. Oestreich, and K. Popp. On the modelling of friction oscillators. *Jounal of Sound and Vibration*, 216(3):435–459, 1998.

[69] S. Oberst, J. C. S. Lai, S. Moore, A. Papinniemi, S. Hamdi, and D. Stanef. Chaos in brake squeal. In *Internoise 2008, Shanghai, 26.-29. October*, 2008.

[70] N.H. Fletcher and T.D. Rossing. *The physics of musical instruments*. Springer-Verlag New York, 1998.

[71] D. Yuhas, J. Ding, and S. Vekatesan. Non-linear aspects of friction material elastic constants. *SEA Technical Papers*, 2006-01-3193:1–10, 2006.

[72] Dassault Systemes. *ABAQUS/CAE User's MANUAL*, 2007.

[73] Surface vehicle recommended practice, disc and drum brake dynamometer squeal noise matrix. Technical report, SAE J2521, 2006.

[74] S. Moore, J.C.S. Lai, S. Oberst, A. Papinniemi, Z. Hamdi, and D. Stanef. Design of experiments in brake squeal. In *Internoise 2008*, 2008.

[75] S Oberst and J.C.S. Lai. Acoustic radiation of instantaneous modes in brake squeal. In *20th International Congress on Acoustics (ICA 2010) in Sydney, 23 - 27 August, Australia*, 2010.

[76] M.F. Jacobson and R. Singh. Acoustic radiation efficiency models of a simple gearbox. Technical report, NASA, Army Research Laboratory, Technical Report ARL-TR-1111, 1996.

[77] F. Fahy and P. Gardonio. *Sound and Structural Vibration: Radiation, Transmission and Response*. Academic Press, Syndey, 2007.

[78] S. Merz. *Passive and Active Control of the Sound Radiated by a Submerged Vessel Due to Propeller Forces*. PhD thesis, University of New South Wales, School of Mechanical and Manufacturing Engineering, 2009.

[79] J. Poblet-Puig, A. Rodriguez-Ferran, C. Guigou-Carter, and M. Villot. Numerical modelling of the radiation efficiency of asymmetrical structures. *Applied Acoustics*, 70:777–780, 2009.

[80] A. Bajer, V. Belsky, and S. Kung. The influence of friction-induced damping and nonlinear effects on brake squeal analysis. *SAE Technical Paper*, 2004-01-2794:1–9, 2004.

[81] D. Guan and J. Huang. The method of feed-in energy on disc brake squeal. *Journal of Sound and Vibration*, 261:297–307, 2003.

[82] Y.S. Kachanov. On the resonant nature of the breakdown of a laminar boundary layer. *Journal of Fluid Mechanics*, 184:43–74, 1987.